Kinetics analysis of chemiluminescence in discharge-driven HF chemical lasers

Wei Luo (罗 威)*, Shengfu Yuan (袁圣付), Baozhu Yan (闫宝珠), Qisheng Lu (陆启生), and Qianjin Zou (邹前进)

College of Opto-electric Science and Engineer, National University of Defense Technology, Changsha 410073, China

**Corresponding author: luowei8786@163.com*

Received February 21, 2011; accepted March 25, 2011; posted online June 16, 2011

The chemiluminescence spectrum in the optical cavity of discharge-driven hydrogen fluoride (HF) chemical laser is measured. The result reveals that the spectra of the helium and fluorine (F) atoms are the major components. Moreover, the green chemiluminescence in the downstream of the optical axis is mostly composed of the 60P20 spectral line of the HF molecule. The analysis shows that, except for the cold pumping reaction, the recombination of the F atoms and the hot pumping reaction also occur in the optical cavity. Due to the hot pumping reaction and the optical cavity temperature in a specific range, the 60P20 line becomes the strongest HF molecule in the downstream region of the optical axis. After the hot pumping reaction, the green chemiluminescence always appears in the downstream region of the optical axis when the optical cavity temperature varies in a greater range.

OCIS codes: 140.1550, 260.1560, 300.6280.

doi: 10.3788/COL201109.081403.

After more than 40 years since their development, the theories and technologies of chemical laser have become more and more comprehensive. Currently, the output power of chemical laser is still the greatest among all lasers. Gain generation assembly is the key element of chemical laser. The mixing performance and the flow field parameters in the optical cavity forming in the gain generation assembly have been studied by numerical simulation[1,2] and experimental diagnostics[3,4]. Spectral analysis of chemiluminescence can give useful information about optical cavities, such as the component of the medium, temperature, kinetics process, and so on[5−7]. In Refs. [8,9], the mixing flowfields and optical gain profiles in hydrogen fluoride (HF) chemical laser systems have been investigated by infrared hyperspectral imaging.

Bright visible chemiluminescence exists in the optical cavity of HF and deuterium fluoride (DF) chemical lasers. According to Ref. [10], the yellow-green chemiluminescence in the HF laser is formed by the 3rd-, 4th-, and 5th-order overtone radiation of the HF molecule[10]. In this letter, we measure the spectrum of the visible chemiluminescence in the HF laser. The chemiluminescence mechanism is then analyzed, and some new ideas are discussed.

An electric discharge-driven continuous-wave (CW) HF laser was used in the experiments. Firstly, NF_3 and the primary helium (He) are injected into the discharge tube after mixing. Fluorine (F) atoms dissociate from the mixed gas through direct current glow discharge. Reaction with H_2 in the gain generation, $F+H_2 \rightarrow HF+H$, produces HF molecules in the vibration excited state to create the population inversions required for lasing. Secondly, He is injected into the end of discharge tube to improve the performance of the laser. N_2 is then injected close to the mirrors to protect them.

Figure 1 shows a photograph of the visible chemiluminescence in the optical cavity. The flow rate of H_2 is about 0.4–0.6 m^3/h when the laser normally works. Whether the H_2 is injected or not, there is always some fluorescence upstream of the optical cavity, which is mostly formed by excited F and He atoms. The interface between the upstream fluorescence and the downstream fluorescence is the contact and reaction region of H_2 and the mixed flow, which contains the F atoms. The velocity of flow in this laser is subsonic; thus, the interface moves upstream when the flow rate of H_2 increases. The downstream fluorescence turns green from yellow when the flow rate of H_2 increases.

The spectrum of the visible chemiluminescence in the HF laser was measured by a fluorescence spectrometer (TRISTAN® light ultraviolet/visible/near-infrared, spectral range: 200–1,100 nm; resolution: 2 nm; wavelength accuracy: 0.1 nm, scan interval used in the measurement: 0.6 nm). The optical axis was 2-mm downstream of the H_2 inject holes, and the flow rate of H_2 was 0.5 m^3/h. Spectral data are presented in Fig. 2. The lines 388.3 (388.9), 446.7, 501.1, 587, 668, 705.9, and 707.1 nm belong to the spectrum of the He atom; the lines 685.5, 690.2, 703.6, 732.7, and 739.7 nm belong to spectrum of the F atom; and the 730.4-nm line may belong to the spectrum of metal electrodes. The 528.3-nm line is

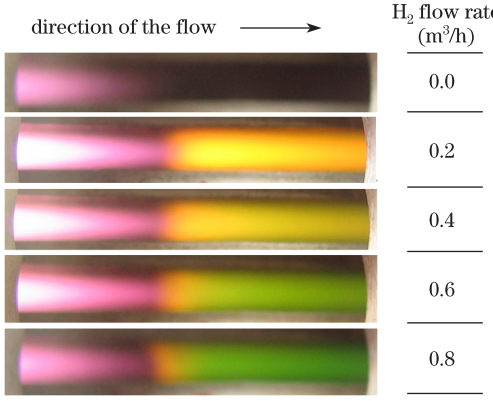

Fig. 1. Photograph of chemiluminescence in the optical cavity.

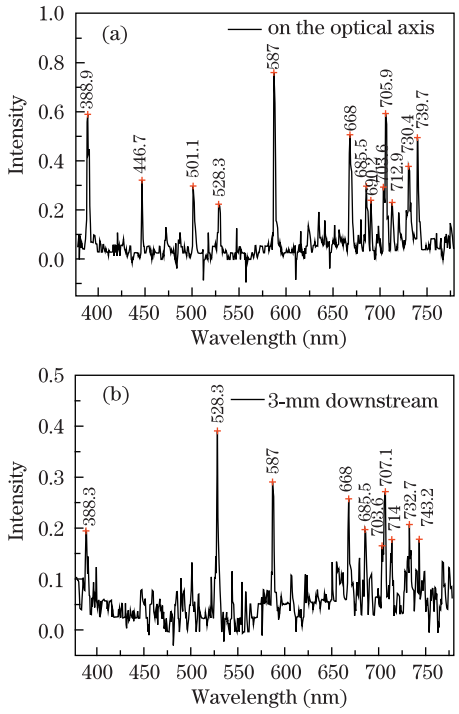

Fig. 2. Spectral data of chemiluminescence in the optical cavity. (a) In the optical axis; (b) 3-mm downstream of the optical axis.

the 60P20 overtone transition of the HF molecule (vibration state: 6–0, rotation quantum number: 20–19). The 528.3-nm line is the only one in green in Fig. 2(b), indicating that the green fluorescence is mostly formed by the 60P20 line of the HF molecule. The wavelengths of the 3–0 vibration state transitions of the HF molecule are in the infrared range. Thus, the finding in Ref. [10] is not accurate. Analyzing the kinetics process in the optical cavity is necessary to explain why only the 60P20 line is obtained among all the overtone lines of the HF molecule.

The major kinetics process in the discharge-driven HF laser is

$$\text{Dissociation reaction:}\quad \mathrm{NF_3} \rightarrow \mathrm{NF_{3-}}_i + i\mathrm{F}. \tag{1}$$

$$\text{Cold pumping reaction:}\quad \mathrm{F} + \mathrm{H_2} \rightarrow \mathrm{HF} + \mathrm{H}. \tag{2}$$

The dissociation reaction in reaction (1) may undergo several reactions to produce the F atom. The highest vibration level that HF molecules can reach is $v = 3$ in reaction (2), and the distribution ratio of HF molecules at the $v = 0 - 3$ level is 0.00:0.15:0.55:0.30[11]. HF molecules at the higher vibration level can be generated by vibration-vibration (V-V) energy transfer:

$$\mathrm{HF}(v=m)+\mathrm{HF}(v=n)\rightarrow\mathrm{HF}(v=m+1)+\mathrm{HF}(v=n-1). \tag{3}$$

Clearly, the populations of the HF molecules at a higher vibration level generated by reaction (3) have the following relationship: $n_{\mathrm{HF}(4)} \gg n_{\mathrm{HF}(5)} \gg n_{\mathrm{HF}(6)}$, where $n_{\mathrm{HF(i)}}$ is the population of the HF molecules at the $v = i$ vibration level. However, the sixth vibration level at the ground level overtone transition is the strongest one in the experiment. Thus, we assume that more kinetics processes exist aside from the process above.

$$\text{F atom recombination:}\quad \mathrm{F} + \mathrm{F} + \mathrm{M} \rightarrow \mathrm{F_2}. \tag{4}$$

$$\text{Hot pumping reaction:}\quad \mathrm{H} + \mathrm{F_2} \rightarrow \mathrm{HF} + \mathrm{F}. \tag{5}$$

Here M denotes the wall or other particles in reaction (4). The hydrogen atom was created through a cold pumping reaction. This indicates that the hot pumping reaction occurs after the cold pumping reaction, usually in the downstream region of the optical axis. The highest vibration level that the HF molecules can reach is $v = 9$ in reaction (5), and the distribution ratio of the HF molecules at the $v = 0 - 9$ level is 0.01:0.02:0.04:0.06:0.11:0.22:0.28:0.14:0.08:0.04. The population of the HF molecules at the $v = 6$ level is the strongest one[11], which is in accordance with the result of the spectrum measurement. Moreover, the exclusive P20 lines can be explained by the gain coefficient calculation of the lines.

For the discharge-driven CW HF/DF chemical laser, the gain coefficient of the spectral line can be expressed as[10]

$$\alpha(v,J,m) = \frac{hcN_{\mathrm{A}}}{4\pi}\left(\frac{W}{2N_{\mathrm{A}}\pi kT}\right)^{1/2} B(v,J,m)(2J+1) \times\left[\frac{n(v')}{Q_{\mathrm{rot}}^{(v')}}\exp\left(-\frac{hc}{k}\frac{E_{v',J+m}}{T}\right)-\frac{n(v)}{Q_{\mathrm{rot}}^{(v)}}\exp\left(-\frac{hc}{k}\frac{E_{v,J}}{T}\right)\right], \tag{6}$$

where v and J are the vibration and rotation quantum number of the low level, and v' and $J+m$ are the vibration and rotation quantum number of the upper level, respectively. For the P-branch transition, $m = -1$; for the R-branch transition, $m = +1$. The partial inversion in the HF/DF laser can lead to gain only in the P branch. h is the Planck constant, N_{A} is the Aphrodite constant, W is the molecular weight of the gain material, $B(v,J,m)$ is the Einstein absorption coefficient, $n(v)$ is the molar concentration of the v vibration level, $Q_{\mathrm{rot}}^{(v)}$ is the rotation level partition function of the v vibration level, c is the speed of light, k is the Boltzmann constant, T is the temperature, and $E_{v,J}$ is the rotation energy of the v and J levels.

Due to the fast deactivation, the excited HF molecules generated by cold reaction mostly come down to the ground state at 3-mm downstream of the optical axis. The real cavity pressure is 0.4 kPa, and the molar concentration of HF is about 10%. Thus, $n(0) \approx 10^{-7}$ mol/cm^3, making $n(6) = \beta n(0)$. Assume that the ratio of the F atom recombination is 20%[12]. Others join the cold pumping reaction; thus, the ratio of F_2 is 10%. The ratio of the HF molecules at the $v = 6$ level generated by the hot pumping reaction is 28%. Assume that only about 30%–40% of the HF molecules at the $v = 6$ level remain 3-mm downstream of the optical axis, resulting from the very fast deactivation of the HF molecule at the high vibration level. Thus $\beta \approx 1\%$.

$Q_{\mathrm{rot}}^{(0)}=0.03381\mathrm{T}; Q_{\mathrm{rot}}^{(6)}=0.0440375\mathrm{T}; Q_{\mathrm{rot}}^{(5)}=0.0419237\mathrm{T}$; and $B(v,J,-1)$. $E_{v,J}$ is a constant corresponding to v and J[10]. By calculating Eq. (6), we can obtain the gain coefficients of the 60P21, 60P20, and 60P19 lines shown in Fig. 3. The weight of the HF molecules at the $v = 5$ level has little difference from that of the HF molecules

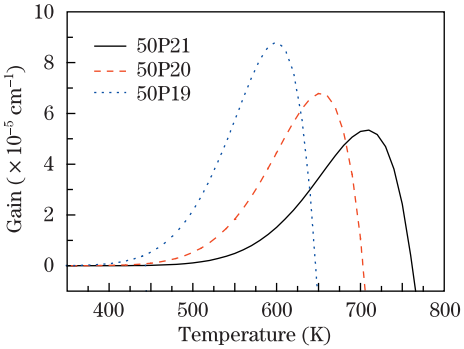

Fig. 3. Gain data of the 60P21, 60P20, and 60P19 spectral lines.

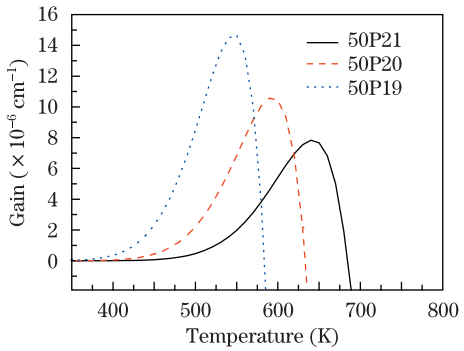

Fig. 4. Gain data of the 50P21, 50P20, and 50P19 spectral lines.

at the $v = 6$ level[11]. Thus, make $n(5) = 0.01n(0)$ as well to obtain the gain coefficients of the 50P21, 50P20, and 50P19 lines shown in Fig. 4.

Figures 3 and 4 show that each line has its own special temperature region, where the gain is larger than the others. For the 60P20 line in Fig. 3, this special region is at 629–683 K, which is reasonable for a subsonic laser[13]. The gain of the lines in Fig. 3 is much larger than the corresponding gain of the lines in Fig. 4. Theoretical calculation of the HF molecule spectral lines shows that the wavelengths of a series of lines from 60P14 to 60P24 are in the green region (560–500 nm). This indicates that if the hot pumping reaction occurs, there will always be a visible green fluorescence in the downstream region of the optical cavity when the temperature of the optical cavity changes in the large region (approximately 350–800 K).

In conclusion, the component and mechanism of chemiluminescence in the HF laser are explained clearly in this letter. The spectral lines of the He and F atoms and the 60P20 line of the HF molecule are the major components of chemiluminescence. Aside from the cold pumping reaction, the recombination of the F atoms and the hot pumping reaction also occurs. The hot pumping reaction and the special temperature of the optical cavity make the intensity of the 60P20 line of the HF molecule strongest in the downstream region.

References

1. T. J. Madden, in *Proceedings of IEEE DoD HPCMP Users Group Conference* 91 (2008).
2. S. P. Jun and W. B. Seung, Int. J. Heat Mass Transfer **49,** 4043 (2006).
3. I. A. Fedorov, M. A. Rotinyan, and A. M. Krivitskii. Quantum Electron. **30,** 1060 (2000).
4. I. A. Fedorov, S. V. Konkin, V. K. Rebone, M. A. Rontinyan, and N. E. Tretyakov, Quantum Electron. **31,** 520 (2001).
5. D. Sun, M. Su, C. Dong, X. Wang, D. Zhang, and X. Ma, Acta Phys. Sin. (in Chinese) **59,** 4571 (2010).
6. C. Han, Y. Liu, Y. Yang, X. Ni, J. Lu, and X. Luo, Chin. Opt. Lett. **7,** 357 (2009).
7. H. Wu, T. Zhu, W. Chen, H. Zhang, and J. Yang. Chin. Opt. Lett. **7,** 542 (2009).
8. S. J. Davis, W. T. Rawlins, D. B. Oakes, G. Dadusc, and D. X. Hammer, in *Proceedings of 34th AIAA Plasmadynamics and Lasers Conference* 3756 (2003).
9. W. T. Rawlins, S. J. Davis, D. B. Oakes, D. X. Hammer, and G. Maislin, in *Proceedings of SPIE Photonics West: Gas and Chemical Lasers,and Applications IV* **5334,** 137 (2004).
10. R. W. F. Gross and J. F. Bott, *Handbook of Chemical Laser* (in Chinese) (Science Press, Beijing, 1987).
11. G. C. Manke II and G. D. Hager, in *Proceedings of 33rd AIAA Plasmadynamics and Lasers Conference* 2219 (2002).
12. J. E. Ferrell, R. M. Kendall, and H. Tong, in *Proceedings of AIAA 6th Fluid and Plasma Dynamics Conference* 0643 (1973).
13. D. J. Spencer, J. A. Beggs, and H. Mirels, J. Appl. Phys. **48,** 1206 (1977).